Advances in Physics Theories and Applications
ISSN 2224-719X (Paper) ISSN 2225-0638 (Online)
Vol.34, 2014

Optical Properties of Semiconducting Pyrite Deposited by Aerosol Assisted Chemical Vapour Deposition (AACVD) Method

Christian Nweze* and Stella Ezeonu
Department of Physics and Industrial Physics, Nnamdi Azikiwe University, P.M.B 5025, Awka, Anambra State, Nigeria.
*E-mail of corresponding author: ci.nweze@unizik.edu.ng

Abstract Semiconducting pyrites were successfully deposited on glass substrates from Diethyldithiocarbamato iron (III) complex (single source precursor) using aerosol assisted chemical vapour deposition (AACVD) method. Structural analysis of the films shows that pure pyrite was deposited at 300°C whereas mixture of pyrite and marcasite was deposited at 350°C, 400°C and 450°C. The concentration of the precursor and deposition time has no visible effect on the structure of the deposited films. Optical analyses of the films show that pure pyrite has higher optical absorbance compared to impure pyrite. The concentration of the precursor and deposited time has significant effect on the optical properties of the deposited films.
Keywords: Pyrite; Marcasite; Diethyldithiocarbamato iron (III); AACVD; XRD; Spectroscopy; Glass substrates.

1. INTRODUCTION

In recent years, synthesis of materials for solar cell application has attracted great interest, more especially cheap and abundant materials with the properties necessary for solar energy conversion. Many of the cheap materials used in solar cell are either non abundant or toxic and as such posed limitations to possible specifically on the potential scale of their usage and applications[1-4] Several physical and electronic properties of iron-sulphide system made them strong candidates for technological application such as solar cells, solid state batteries [5] and catalysis [6]. There are various phases of iron-sulphide systems; they are pyrite (Cubic FeS_2), marcasite (calcium chloride structure-FeS_2), troilite (FeS), mackinawite ($Fe_{1+x}S$), pyrrhotite ($Fe_{1-x}S$, Fe_7S_8), smythite (hexagonal Fe_3S_4) and greigite (cubic spinel-Fe_3S_4) [3-5]. The phase of iron-sulphide system that is formed is a function of how the material is formed e.g. the precursors used and specifically the temperatures of the reaction[5] while the stoichiometry ratio of iron and sulphur determines the structure[3]. Pyrite (Cubic FeS_2) seems to be the better candidate for solar cell application due to its earth abundance, cheap and non-toxic material even with its low solar energy conversion efficiency[3,7,8]. Pyrite has some properties that make it suitable for Photovoltaic (PVs) application, these solid state properties include, indirect band gap of 0.98eV, optical absorption coefficient of $10^5 cm^{-1}$(for λ <900 nm), adequate minority carrier diffusion length of (100-1000) nm, high photocurrent and high quantum efficiencies [8-10]. Various methods have been used to deposit pyrite, such as, chemical spray pyrolysis[11], vapour transport[12], vacuum thermal evaporation[13], hot injection method[1], sulphurization of iron oxides[14], ion beam and reactive sputtering [15], and plasma assisted sulphurization of iron[16]. In this research work, we used solution based method, precisely Aerosol Assisted Chemical Vapour Deposition (AACVD) method to deposit nanocrystals of Pyrite from a solution using single source precursor and characterized the deposited films using XRD and UV – VIS spectrometer in other to determine the structure and optical properties of pyrite respectively.

2. EXPERIMENTAL

All reagents were used as purchased and solvents were distilled prior to use. All syntheses were performed under an inert atmosphere of dry nitrogen using standard schlenk techniques. Elemental analysis was performed by the University of Manchester micro-analytical laboratory. Mass spectra were recorded on a Kratos concept 1S instrument. Infra-red spectra were recorded on a Specac single reflectance ATR instrument (4000-400 cm^{-1}, resolution 4 cm^{-1}). Melting points were recorded on a Barloworld SMP10 Melting Point Apparatus. p-XRD studies were performed on an Xpert diffractometer using Cu-Kα radiation. The samples were mounted flat and scanned between 20° and 70° with a step size of 0.05° and various count rates. Absorbance spectra data of the films were obtained using Agilent HP8453 UV – VIS spectrophotometer. From the absorbance, various other optical parameters which include: Optical band gap, Refractive index, Coefficient of absorption, and Optical conductivity were derived.

2.1 Precursor synthesis

Following the procedure of Masood *et al* 2011, Diethyldithiocarbamato iron (III) was prepared[17].

2.2. Preparation of solution

The solutions were prepared by dissolving different masses of the precursor ($FeS_2CN(Et)_2)_3$) in toluene. 0.3g (0.6 mmol), 0.15g (0.3 mmol) and 0.075g (0.15 mmol) of the precursor were separately dissolved in 15ml toluene in

a two-necked 100ml round bottom flask and concentrations of 0.04mol/dm3, 0.02mol/dm3 and 0.01mol/dm3 respectively were achieved. The substrates used were glass microscope slides. The glass slides were cut to size approximately 1 x 2 cm^2 by hand. The substrates were not handled with bare fingers rather with hand gloves to avoid contamination. The substrates were cleaned with detergent solutions, rinsed with distilled water and then rinsed with acetone, methanol and distilled water and finally dried before use.

2.3. Deposition of thin films of Pyrite by AACVD

15ml of the solution was poured into the two-necked round bottom flask with a gas inlet that allowed argon (carrier gas) to pass into the solution to aid the transport of the aerosol. A piece of reinforced tubing was used to connect the flask to the reactor tube. Platon flow gauge was used to control argon flow rate. Seven glass substrates (approximately 1 x 2 cm^2) were placed inside the reactor tube which is placed in a Carbolite furnace maintained at a certain temperature. The precursor solution in a two-necked round bottom flask was kept in a water bath above the piezoelectric modulator of a PIFCO ultrasonic humidifier (Model No 1077). The solution was evaporated and the generated aerosol droplets of the precursor were transferred into the hot wall zone of the reactor by the carrier gas. This precursor vapour reached the heated substrate surface where thermally induced reactions and film deposition took place at a particular time and temperature. **Tables 1, 2 and 3** summarized the parameters that were varied during the deposition.

S/N	Slide No	Argon flow rate (sccm)	Concentration of precursor (mol/dm^3)	Temperature of deposition (^oC)	Time of deposition (minutes)	Repeated times
1	M	160.00	0.04	300.00	30.00	3
2	N	160.00	0.04	300.00	60.00	3
3	O	160.00	0.04	300.00	120.00	3

Table 1 The variation of time while keeping other parameters constant

S/N	Slide No	Argon flow rate (sccm)	Time of deposition (minutes)	Temperature of deposition (^oC)	Concentration of precursor (mol/dm^3)	Repeated times
1	P	160.00	60.00	300.00	0.04	3
2	Q	160.00	60.00	300.00	0.02	3
3	R	160.00	60.00	300.00	0.01	3

Table 2 The variation of concentration while keeping other parameters constant.

S/N	Slide No	Argon flow rate (sccm)	Concentration of precursor (mol/dm^3)	Time of deposition (minutes)	Temperature of deposition (^oC)	Repeated times
1	E	160.00	0.04	60.00	300.00	3
2	F	160.00	0.04	60.00	350.00	3
3	G	160.00	0.04	60.00	400.00	3
4	H	160.00	0.04	60.00	450.00	3

Table 3 The variation of temperature while keeping other parameters constant

3. RESULTS AND DISCUSSION

The **p-XRD** patterns of the deposited films are shown in **figures 1 and 2**. **Figure 1** shows that films deposited at 300^{o}C and varying concentration and time correspond to pure cubic pyrite ($FeS_{1.96}$ (ICDD No. 01-073-8127)) phase. (111), (200), (210), (211), (220), (311) and (321) planes of reflection were dominant at all depositing time and concentration. **Figure 2** shows that pure pyrite is formed at 300^{o}C but a mixture of pyrite and some peaks corresponding to marcasite (ICDD No. 04-003-2016) is formed at 350^{o}C, 400^{o}C, and 450^{o}C. Again it is observed that (200) plane of reflection is the preferred orientation of the crystals at any depositing temperature. The optical absorbance of the deposited iron sulphide films in the photon energy range of 1.3eV – 4.2eV has been investigated using Agilent HP8453 UV-VIS spectrophotometer. **Figures 3, 4 and 5** show the plot of optical absorbance against the photon energy. The films show significant absorbance in high photo energy whereas the absorbance decreased as the photon energy decreases. From **figure 3**, it is observed that the absorbance of the pure pyrite films increased with deposition time because of the increase in the thickness of the deposited films. It is also observed that the absorbance increased with increase in the concentration of the precursor (**figure 4**). The absorbance of impure pyrite is seen to be generally lower than that of pure pyrite as shown in **figure 5**. The absorbance of pyrite indicated that the films are active in the visible and infra-red region, thus there is possibility that this material can be used as either infrared devices or solar cells.

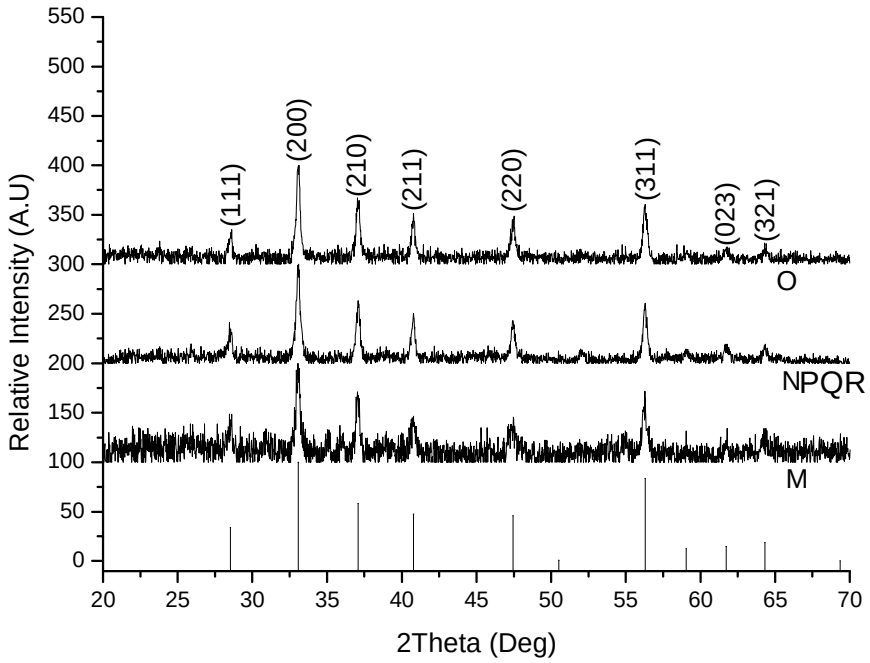

Figure 1. p-XRD pattern of the deposited films at various concentration and time (slides O, N, P, R, and M). The figure shows that polycrystalline pyrite is formed with planes of reflection on (111), (200), (210), (211), (220), (311) and (023). The vertical lines represent standard p-XRD pattern of cubic pyrite ($FeS_{1.96}$ (ICDD No. 01-073-8127))

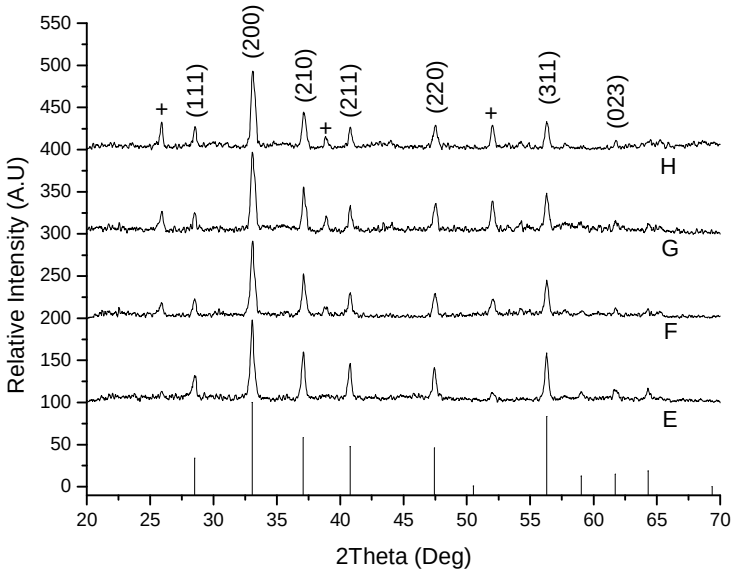

Figure 2. p-XRD patterns of deposited films, at 300^{o}C (slide E) pure polycrystalline pyrite ($FeS_{1.96}$ (ICDD No. 01- 073-8127) is formed with planes of reflection on (111), (200), (210), (211), (220), (311) and (023), at 350^{o}C (slide F), 400^{o}C (slide G), 450^{o}C (slide H) mixture of pyrite and marcasite (+) (ICDD No. 04-003-2016).

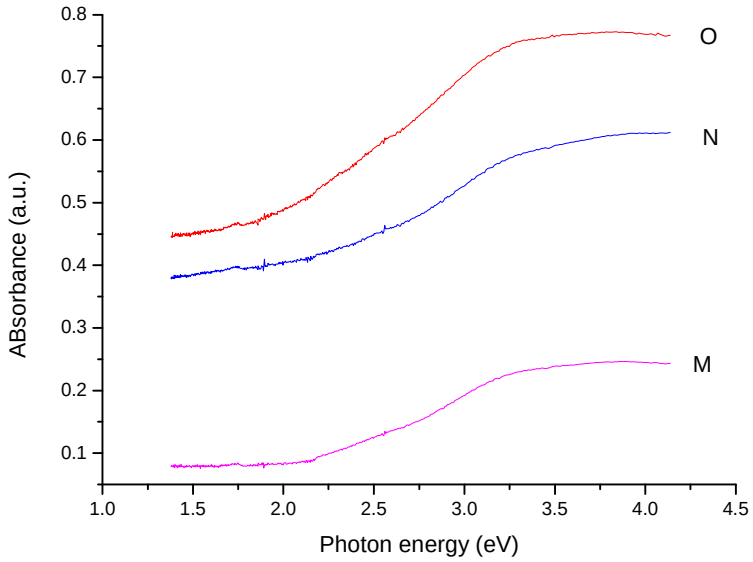

Figure 3. Plot of absorbance against photon energy (slides O, N, M)

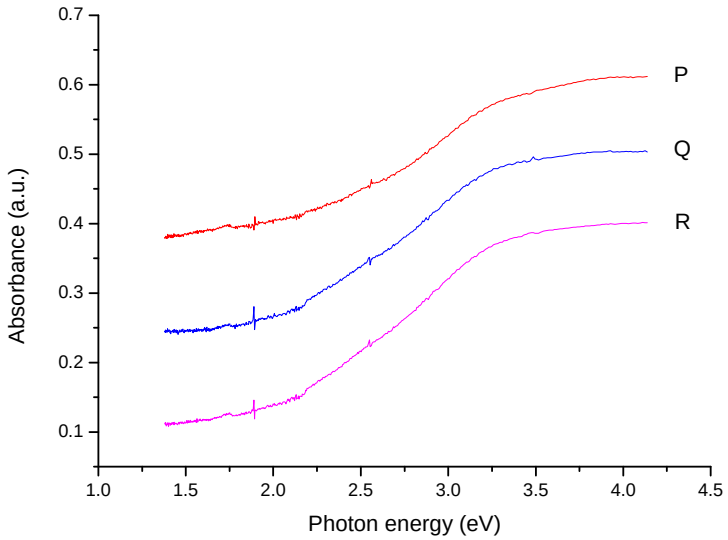

Figure 4. Plot of absorbance against photon energy (slides P, Q, and R)

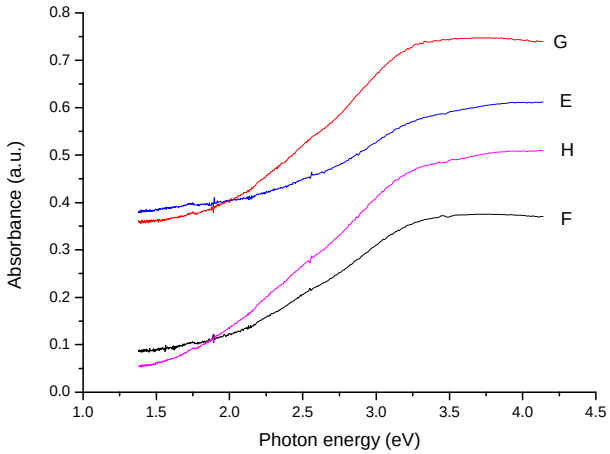

Figure 5. Plot of absorbance against photon energy (slides E, F, G, and H)

Figures 6 shows the plot of absorption coefficient squared (α^2) versus photon energy (**eV**) of the deposited pyrites (pure and impure). Extrapolation of the straight portion of the graph touches the photon energy at 2.0eV. Therefore the direct band gap of the deposited film is 2.0eV, this bang gap compares well with direct band gap of 1.85eV reported by Anuar *et al*, (2010)[18]. The increase in the band gap of the films, from 0.98eV for indirect band gap to 2.0eV for direct band gap[1], is as a result of phonon contributions[19,20]. The optical conductivity of the pyrites was estimated using $\sigma_0 = \frac{\alpha n c}{4\pi}$ (**figures 7, 8 and 9**). The figures showed that pure pyrite has high optical conductivity than the impure pyrite. The optical conductivity increased with the photon energy for both pure and impure pyrites and as such pyrite might be considered as nice glazing materials for maintaining cool interior in building in warm climate region while keeping the rooms well illuminated.

Figures 10, 11 and 12 showed the plot of refractive index against photon energy. From **figure 10**, it is observed that the pyrite film deposited under 300^{o}C and 30mins (slide M) has high refractive index of about 2.6 in high photon energy and refractive index of about 1.8 in lower photon energy whereas the reverse is the case for films deposited 300^{o}C, 60mins and 120mins. Films deposited at 60mins (slide N) and 120mins (slide O) have approximately refractive index of 2.6 in lower photon energy and refractive index of 2.25 and 1.60 respectively at high photon energy. The figure also shows a transition photon energy (2.0eV – 3.25eV) through which the refractive index changes from high value to low value and vice versa.

Figure 11 shows that concentration of the precursor has an effect on the refractive index of the deposited films. The film deposited under 300°C, 60mins and 0.01mol/dm3 of the precursor (slide R) shows high refractive index of 2.65 and 2.00 at high and low photon energy respectively. The film deposited under 300°C, 60mins and 0.02mol/dm3 of the precursor (slide Q) has peak value of refractive index of 2.65 at photon energy of 2.75eV but the refractive index decreased as the photon energy is decreased or increased above 2.75eV. The film deposited under 300°C, 60mins and 0.04mol/dm3 (slide P) shows refractive index of 2.65 at low photon energy and refractive index of 2.25 at high photon energy.

Figure 12 shows the effect of temperature on the refractive index of the deposited films. The films deposited at 300°C (slide E) and 400°C (slide G) show low refractive index at high photon energy and high refractive index at low photon energy. The films deposited at 350°C (slide F) and 450°C (slide H) show high refractive index at high photon energy and low refractive index at low photon energy.

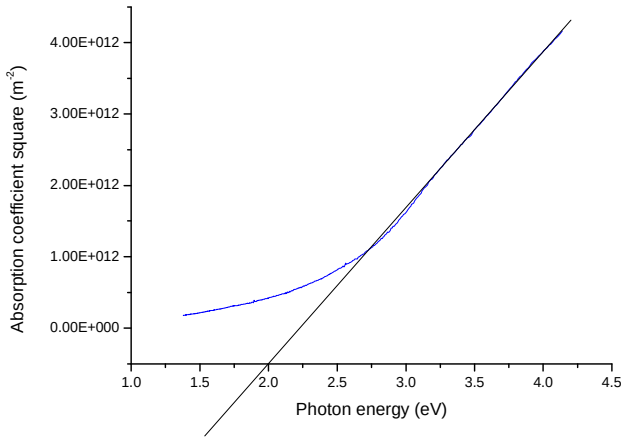

Figure 6. Plot of absorption coefficient square against photon energy

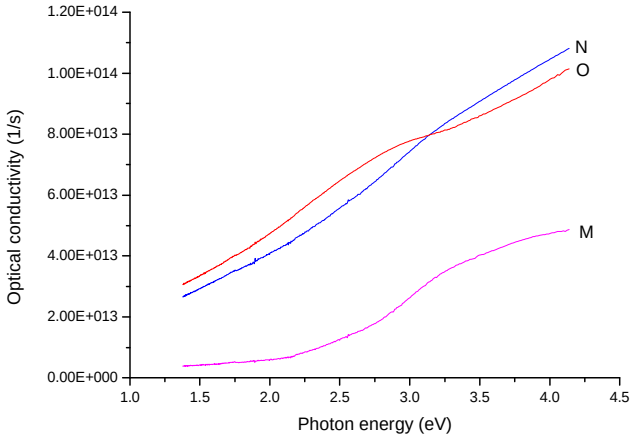

Figure 7. Plot of optical conductivity against photon energy (slides N, O, and M)

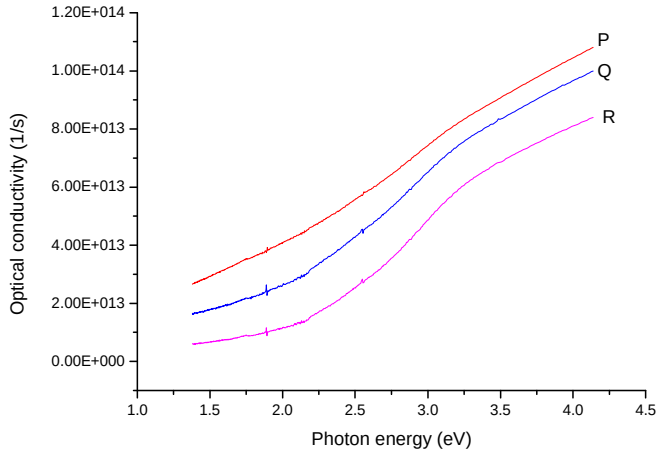

Figure 8. Plot of optical conductivity against photon energy (slides P, Q, and R)

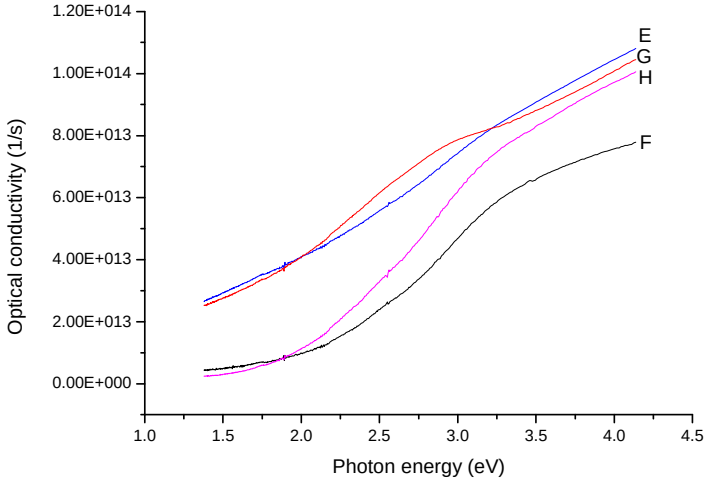

Figure 9. Plot of optical conductivity against photon energy (slides E, F.G, and H)

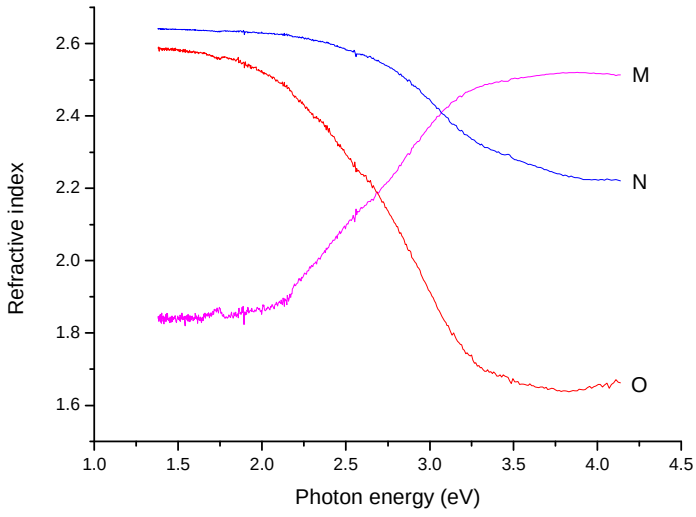

Figure 10. Plot of refractive index against photon energy (slides M, N, and O)

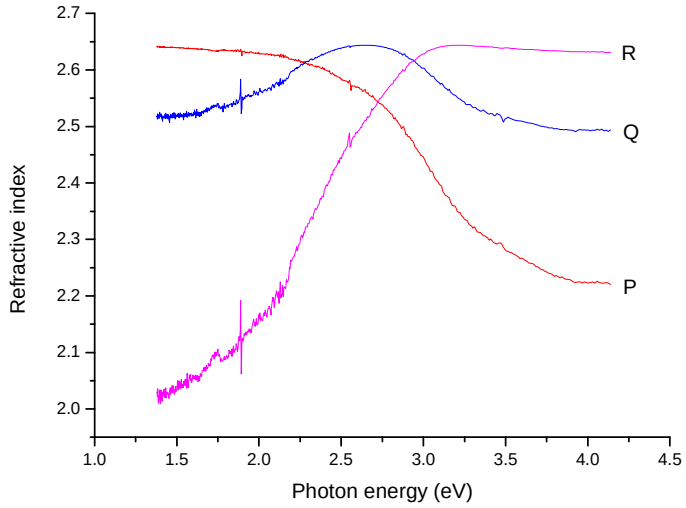

Figure 11. Plot of refractive index against photon energy (slides R, Q, and P)

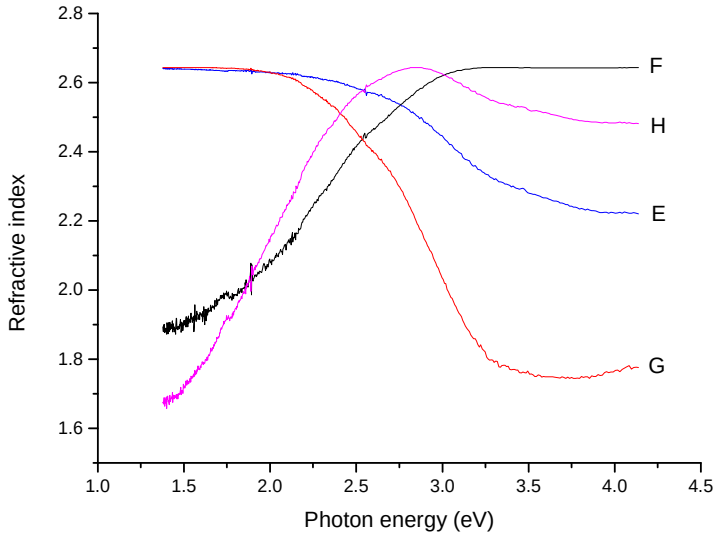

Figure 12. Plot of refractive index against photon energy (slides F, H, E, and G)

4. CONCLUSION

Semiconducting pyrite was successfully deposited from a single source precursor using AACVD. The concentration of the precursor and deposition time has no visible effect on the crystal structure of the films whereas the temperature of deposition affects the phase of the iron sulphide that is formed. Pure polycrystalline pyrite is formed at 300^{o}C with preferred orientation lying on (200) plane of reflection whereas mixture of pyrite and marcasite is formed at 350^{o}C, 400^{o}C and 450^{o}C. Optical analysis shows that pure pyrite has higher optical absorbance than impure pyrite. The absorbance, refractive index and optical conductivity are affected by the concentration of the precursor used and time of deposition.

ACKNOWLEDGEMENT

The authors are grateful to Tertiary Education Trust Fund (TETFund) for sponsoring this research work. Many thanks to Dr. Chris Wilkinson, Michael Faulkner and Gary Harrison of the University of Manchester for their time in training us on how to use various machines in the school of material sciences.

REFERENCE

1. Steinhagen Chet, Taylor B. Harvey, C. Jackson Stolle, Justin Harris, and Brian A. Korgel. (2012). Journal of Physical Chemistry Letters. 3, 2352.
2. Wadia C, Alivisatos A.P, Kammen D.M. (2009). Environ. Sci. Technol. 43, 2072.
3. Masood Akhtar, Ahmed Lufti Abdelhady, M. Azad Malik, and Paul O'Brien. (2012). Journal of Crystal Growth. 346, 106.
4. Ennaoui A and Tributsch H. (1984). Sol. Cells. 13, 197.
5. Barnard Amanda and Russo Salvy. (2009). Nanotechnology. 20, 115702
6. ang S.S. and Seefurth R.N. (1987). J. Electrochem. Soc. 134, 530.
7. Ahmed Lufti Abdelhady, Mohammad A. Malik, Paul O'Brien and Floriana Tuna. (2012). Journal of Physical Chemistry. 116, 2253.
8. Hopfner C, Ellmer K, Ennaoui A, Pettenkofer C, Fiechter S, Tributsch H. (1995). Journal of Crystal Growth.151
9. Puthussery James, Sean Seefeld, Nicholas Berry, Markelle Gibbs and Matt Law. (2011). Journal of the American Chemistry Society. 133, 716.
10. Ramasamy K., Malik M.A., Helliwell M., Tuna F., and O'Brien P. (2010). Inorganic Chemistry 49, 8495.
11. Smestad G, Da Silva A, Tributsch H, Fiechter S, Kunst M, Meziani N, Birkholz M. (1989). Solar Energy Materials. 18, 299.
12. Ennaoui A, Schlichtlorel G, Fiechter S, Tributsch H. (1992). Solar Energy Materials and Solar Cells. 25, 169.
13. Re Zig B, Dalma H, Kanzai M. (1992). Renewable Energy. 2, 125.
14. Ouertani B, Ouerfelli J, Saadoun M, Bessais B, Ezzaouia H, Bernede J.C. (2005). Material Characterization. 54, 431.
15. Birkholz M, Lichtenberger D, Hopfner C, Fiechter S. (1992). Solar Energy Materials and Solar Cells. 27, 243.
16. Bausch S, Sailer B, Keppner H, Willeke G, Bucher E, Frommeyer G. (1990). Applied Physics Letters. 25, 57.
17. Masood Akhtar, Javeed Akhter, Azad Malik, Paul O'Brien, Floriana Tuna, James Raftery and Madeleine Helliwell (2011), Journal of material chemistry. 21, 9737.
18. Anuar Kassim, Tan WeeTee, Dzulkefly Kuang Abdullah, Atan Mohd Sharif, Ho SoonMin, Gwee Siew Yong and Saravanan Nagalingam. (2010). Indo. J. Chem. 10(1), 8.
19. Moss T.S. (1961). Optical properties of semiconductors, Butterworth and Pub. Ltd. London 2.
20. Harbeke G. (1972). Optical properties of semiconductors, North-Holland Pub. Co. Amsterdam. 398.

The IISTE is a pioneer in the Open-Access hosting service and academic event management. The aim of the firm is Accelerating Global Knowledge Sharing.

More information about the firm can be found on the homepage:
http://www.iiste.org

CALL FOR JOURNAL PAPERS

There are more than 30 peer-reviewed academic journals hosted under the hosting platform.

Prospective authors of journals can find the submission instruction on the following page: http://www.iiste.org/journals/ All the journals articles are available online to the readers all over the world without financial, legal, or technical barriers other than those inseparable from gaining access to the internet itself. Paper version of the journals is also available upon request of readers and authors.

MORE RESOURCES

Book publication information: http://www.iiste.org/book/

IISTE Knowledge Sharing Partners

EBSCO, Index Copernicus, Ulrich's Periodicals Directory, JournalTOCS, PKP Open Archives Harvester, Bielefeld Academic Search Engine, Elektronische Zeitschriftenbibliothek EZB, Open J-Gate, OCLC WorldCat, Universe Digtial Library , NewJour, Google Scholar